Contribution from the Laboratorio di Tecnologia dei Materiali, C.N.E.N., Roma, Laboratorio di Chimica e Tecnologia dei Materiali e dei Componenti per l'Elettronica, C.N.R. Bologna, and Istituto Chimico G. Ciamician, Università di Bologna, Italy

X-Ray Diffraction Investigations on the Structure of some Thoria Gels

A. Cabrini,* G. Celotti, and R. Zannetti*****

Received October 26, 1970

The structure of some samples of thoria gels has been investigated by X-ray small-angle diffraction and by radial electronic distribution analysis, performed through elaboration of wide-angle spectra. The presence of colloidal particles has been revealed, tending to spherical shape, which have nearly equal dimensions in samples which were not treated at high temperatures. Such particles are formed by a core of oxide, coated by a hydroxyl groups shell, located in the three (0,0,½) interstitial positions of the cubic face-centered lattice (fluoryte type), and by water molecules on a more external layer, which contributes to the formation of bonds between the different particles. The average particles dimensions, their polydispersity and the order degree in the oxide core may largely change with preparation procedures of gels and with annealing temperature.

Introduction

During some researches carried out by C.N.E.N. in order to characterize sols and gels of metal oxides of nuclear interest,[1] some investigations on crystallization kinetics of ThO_2 and on the activation energy and growing mechanism of its particles in different kinds of gels as a function of the temperature and of the annealing time have been performed. The results of these studies have been already published.[2]

The structure of the gels of metal oxides is however still little known: measurements of crystallite and particle dimensions in fresh sols and gels and of the average lattice parameters have been performed. In particular, for the short-range array only suppositions have been formulated:[3] it has been proposed that these materials are composed of hydrated oxy-hydroxides analogous to those of trivalent metals that are found in nature as minerals (diaspore, goethite, boehmite), which have been also prepared by synthesis.[4-6]

In nature, hydrated oxides of thorium and uranium at an oxidation number of 4+ are unknown and attempts to obtain them by synthesis have been unsuccessful.[6,7] The compound $UO(OH)_2$, face centered cubic, has been prepared but not sufficiently characterized by Glemser.[8]

We have better information on the long-range structure: the studies have been essentially directed towards the knowledge of colloidal particles, in order to determine the average dimensions and the shape and distribution of diameters by X-ray small-angle diffraction methods.[9-11]

In this work, carried out in collaboration between C.N.E.N. and the departments of structural chemistry of the University and C.N.R. of Bologna, the contribution to this research by X-ray diffraction methods is described, and some results which make possible a classification valid in general for such materials are reported.

Experimental Section

Apparatus and samples. X-ray diffraction measurements at small and wide angles have been carried out: for the former we employed a model I Rigaku-Denki camera and a Kratky camera, both working with copper X-radiation and counter detector. For wide angles measurements a Philips diffractometer was used, equipped with proportional counter, pulse height analyzer and potentiometric recorder. Ni-filtered copper radiation has been used and about 80% of X-ray path has been evacuated in order to reduce the air scattering.

Diffracted intensities at various θ Bragg angles have been directly measured on the recording chart with the goniometer working at a low scanning speed. The details on the features of small-angle measurements have been already reported in previous works[12-13] to which we refer to for all further information on this technique.

(*) Laboratorio di Tecnologia dei Materiali - C.N.E.N. (Comitato Nazionale per l'Energia Nucleare), Centro Studi Nucleari della Casaccia, Roma.
(**) Laboratorio di Chimica e Tecnologia dei Materiali e dei Componenti per l'Elettronica - C.N.R. (Consiglio Nazionale delle Ricerche), Bologna.
(***) Istituto Chimico « G. Ciamician » della Università di Bologna.

(1) M. Zifferero - *Comit. Naz. Energ. Nucl.*, RT/*CHI* (68) 28 (1968).
(2) G. Scibona, A. Bazzan, A. Cabrini, R. Chiarizia, P. R Danesi, M. Magini, and E. Mezi, *Atti del Simposio Nucleare*, Torino, 2 October 1967.
(3) R. De Leone, *Comit. Naz. Energ. Nucl.*, DiChi (65) 23 (1965).
(4) W. O. Milligan, *J. Phys. Chem.*, *60*, 273 (1956).
(5) R. A. Laudise, *J. Am. Chem. Soc.*, *81*, 562 (1959).
(6) O. Glemser, *Angew. Chem.*, *73*, 785 (1961).
(7) A. Bazzan, private communication.
(8) O. Glemser, *Angew. Chem.*, *73*, 795 (1961).
(9) P. W. Schmidt, *J. Phys. Chem.*, *69*, 3849 (1965).
(10) W. C. Stoecker, *Anal. Chem.*, *39*, 628 (1967).
(11) A. Cabrini, G. Celotti, R. Zannetti, *Comit. Naz. Energ. Nucl.* RT/MET (68) 1 (1968).
(12) R. Zannetti, A. Fichera, G. Celotti, A. Ferrero Martelli, *Eur. Polymer J.*, *4*, 399 (1968).
(13) O. Kratky - in « Small-angle X-ray scattering », H. Brumberger (Ed.), Gordon & Breach, New York, 1967, p. 63.

The examined ThO_2 gels have been prepared by the method described by Cogliati and coworkers.[14] The starting concentration of thorium nitrate solution used to prepare the sols was about 4 moles/liter.

The precipitation process has been carried out in three different ways:

(a) at room temperature;

(b) by ageing of the sol at 80°C and precipitation at room temperature;

(c) at 80°C.

Samples of this last gel annealed at 120°C for 24 hours and at 400°C for 8 hours were also examined.

The gels obtained in the three above described ways have been investigated by small- and wide-angle diffraction techniques, determining the average dimensions of the crystallites which amount to 20, 30, and 50 Å, and the average dimensions of the colloidal particles of 25, 30, and 70 Å respectively.

Furthermore three series of annealed gels have been prepared, later indicated as C1, C2, and C3, through gradual annealing up to 1100°C of the samples LC, MC, and HC (see below).

The examined specimens will be later indicated on the basis of their crystallite size and of the above described preparation methods, as LC (low crystallinity), MC (medium), HC (high), HC/120° and HC/400°. Their densities were 4.40, 4.86, and 5.32 g/cm³, corresponding to 45, 49, and 54% if compared with crystalline ThO_2 ($\rho = 9.84$ g/cm³) for the first three unannealed samples, and 6.0 and 8.1 g/cm³ (61 and 82%) for the annealed ones.

The chemical analysis showed the presence of 0.10-0.25 NO_3^- residual groups per thorium atom: the results of the analysis of the examined samples are summarized in Table I

Table I. Analytical data for examined samples. Data obtained from chemical and thermogravimetric analyses and from specific weight measurements in CCl_4. Average stoichiometric formula for gels: $ThO(OH)_{2-x}(NO_3)_x$.

	LC % weight	MC % weight	HC % weight	HC/120° % weight	HC/400° % weight
Th^{4+}	34.42	36.92	40.59	41.78	80.90 (ThO_2)
O^{2-}	2.36	2.52	2.79	3.00	
NO_3^-	1.12	0.99	2.72	2.29	«0.2
OH^-	4.75	5.16	5.23	5.25	n.d.
H_2O	57.35	54.41	48.67	47.68	19.10

Diffractometric studies of particles. As in the above mentioned work,[11] for the small-angle method we followed the Hosemann-Bagchi treatment[15] and in particular the Hosemann-Joerchel procedure.[16]

A good agreement between small- and wide-angle methods has been found for all the freshly prepared gels; the correlation is worse in the case of dried samples, depending on annealing time and especially temperature.

According to Hosemann treatment, the average intensity diffracted by a system of globular polydispersed particles, can be expressed as sum of three terms:

$$\bar{I}(\vec{b}) = \bar{I}_c(\vec{b}) + \bar{I}_p(\vec{b}) + \bar{I}_f(\vec{b}) \qquad (1)$$

where $\bar{I}_c$ and $\bar{I}_p$ are respectively the components of the volume and particle scattering, while $\bar{I}_f$ is the interference correction term.

For closely packed materials this term presents noticeable relevance since it produces a displacement to wider angles of the experimental curve of diffracted intensity, so that smaller dimensions than the true ones are determined for the particles. We use the symbols of Hosemann[15] for this correction, function of the packing density ε^3 and of the polydispersity g_y. The quantity ε^3 is considered equal to the ratio between the actual density of the gel and that of crystalline ThO_2; however, in the case of substances with an inflexion point in the scattering curve, we have:

$$g_y \cong \varepsilon^3$$

Applying the correction formula to the experimental $(u_m)_{obs}$ value (where $u = |\vec{b}| = 2 \sin\theta/\lambda$) determined according to Hosemann-Joerchel treatment, we have:

$$u_m = (u_m)_{obs}\left[1 + \frac{\varepsilon^3}{3}(1 + 2g_y^2)\right]^{-1} \qquad (2)$$

This value u_m is always smaller than the experimental one, and the average particles diameter:

$$2\bar{r} = \frac{0.96}{\pi u_m} \cdot \frac{9.6 - 2M^*}{\sqrt{7.5 - M^*}} \qquad (3)$$

(where $M^* = u_o/u_m$) results higher than the uncorrected one.

In materials not presenting inflexions in the scattering curve, ε^3 is determined by the above mentioned method and g_y is derived from:

$$g_y = \sqrt{\frac{M^* - 2.1}{9.6 - 2M^*}} \qquad (4)$$

where M^* is the effective value determined from the graph u^2I *vs.* u.

In any case it is possible to correct M^* through:

$$M^* = (M^*)_{obs}\left[1 + \frac{\varepsilon^3}{4}(1 - 2g_y^2)\right] \qquad (5)$$

and by means of these new values of ε^3, u_m and M^* to evaluate also the actual elongation, polydispersity, mass statistics and specific surface.

The above described methods have been applied to the three series of annealed gels C1, C2, and C3 (see Tables II, III, and IV for detailed characteristics).

The samples of the first group present no inflexion in the scattering curve at small angles, while those of the other two groups, except the unannealed ones, show more or less evident inflexions and in this case the setting $g_y \cong \varepsilon^3$ is correct.

(14) G. Cogliati, R. De Leone, R. Lanz, and G. Scibona - *A/Conf.* 28/P/555 ICPUAE Geneva, September 1964.
(15) R. Hosemann, and S. N. Bagchi, *Direct Analysis of Diffraction by Matter*, North-Holland, Amsterdam, 1962.
(16) D. Joerchel, *Zs. Naturforschg., 12 a*, 123 (1957).

Table II. Average crystallites and particles dimensions for samples C1. Notes: columns 1 and 2: annealing temperature and time; 3: polydispersity; 4: experimental packing density from density measurements; 5: average diameters of particles (Å) without interference correction; 6: the same, but with interference correction applied; 7: average crystallites dimensions (in Å) from peak broadening measurements, under the hypothesis of gaussian-shaped profiles.

Samples 1 °C	2 hours	g_y 3	ε^3 4	$2\bar{\bar{y}}$ 5	6	η 7
r.t.	—	0.10	0.20	20	20	30
200	10	0.30	0.35	25	25	30
500	10	0.46	0.55	35	40	60
800	2	0.71	0.82	90	140	145
800	6	0.78	0.82	110	175	180
800	10	0.79	0.82	115	185	200
1100	2	0.54	0.94	250	375	360
1100	6	0.60	0.94	260	410	415
1100	10	0.61	0.94	270	430	460

Table III. Average crystallites and particles dimensions for samples C2. Notes: columns 3 and 4: polydispersity has been in this case put equal to packing density, $g_y \cong \varepsilon^3$. Headings of the columns are the same as in Table II.

Samples 1 °C	2 hours	$g_y(\cong\varepsilon^3)$ 3-4	$2\bar{\bar{y}}$ 5	6	η 7
r.t.	—	0.20	20	25	20
400	10	0.60	50	70	45
800	0.2	0.90	140	190	180
1000	0.2	0.94	370	655	625
1000	24	0.96	420	840	945
1000	32	0.96	470	985	1010

Table IV. Average crystallites and particles dimensions for samples C3. Headings of columns are the same as in Tables II and III.

Samples 1 °C	2 hours	$g_y(\cong\varepsilon^3)$ 3-4	$2\bar{\bar{y}}$ 5	6	η 7
r.t.	—	0.20	70	75	30
400	10	0.60	30	45	40
700	0.2	0.85	55	95	55
800	0.2	0.87	65	110	90
800	2	0.87	105	180	130
1000	0.2	0.90	130	225	235
1000	2	0.90	165	290	420
1100	0.1	0.93	180	330	410

In all the cases, ε^3 is an experimental value, depending on density; the most correct values are obtained when the above mentioned approximation is valid, as the value g_y of (4) is affected by errors in the evaluation of u_o and therefore of M^*.

In Tables II, III, and IV the average diameters of particles are reported and then compared with the average dimensions of crystallites as determined by wide-angle diffraction, following the Scherrer method in which the average crystallite size η determines the value of the half-peak broadening β_1, according to:

$$\beta_1 = \frac{K\lambda}{\eta \cos\theta} \tag{6}$$

(where λ = wavelength of the X-radiation and K is a constant whose commonly used[17] value is about 0.9).

The lattice distortions $\delta a/a$ yield a further broadening β_2 that may be calculated for cubic substances[18] from:

$$\beta_2 = 4\frac{\delta a}{a}\tan\theta \tag{7}$$

where a is the value of the unit cell parameter.

According to Hall,[19] the broadenings β_1 and β_2 produced by these two phenomena are additive, that is:

$$\beta_c = \beta_1 + \beta_2 = \frac{K\lambda}{\eta\cos\theta} + 4\frac{\delta a}{a}\tan\theta \tag{8}$$

or:

$$\beta_c\cos\theta = \frac{K\lambda}{\eta} + 4\frac{\delta a}{a}\sin\theta \tag{8'}$$

Therefore by plotting $\beta_C \cos\theta$ in function of $\sin\theta$, a straight line is obtained whose intercept on the ordinates axis gives η and whose slope $\delta\, a/a$.

The simple additiveness of the broadening effects is really rather questionable: it would be correct if the shape of the peaks could be represented as a Cauchy function $f(x)=(1+k^2x^2)^{-1}$.

If on the contrary the profile approaches a gaussian curve, that is $f(x)=(1+k^2x^2)^{-2}$, the additiveness of the squares of β_1 and β_2 should be more correct and the plot should report $\beta_C^2\cos^2\theta$ in function of $\sin^2\theta$, with $\beta_C = \beta_1^2 + \beta_2^2$.

According to some authors, including Warren,[20] if the broadening produced by crystallite size is prevalent, a Cauchy-type behaviour is obtained, while the contribution of the deformations can be better expressed by a gaussian curve; therefore the simplified addition process is not quite correct.

For materials having features analogous to ThO_2, as for example uranium oxide modified through irradiation,[21] it has been demonstrated that the broadenings may be represented by a gaussian curve; as a first approximation we can indeed consider the hypothesis of square additiveness to be correct in our case.

For the samples of C1 series we have also calculated the average dimensions of crystallites with the method handling experimental profiles by Fourier analysis, according the procedures of Stokes,[22] performing mathematical elaboration with the aid of an IBM 360 computer and separating the contributions of deformations.[23] In this case we observed that the best agreement between $2\bar{\bar{y}}$ values and those evaluated for crystallite sizes by the three above mentioned methods are obtained from the hypothesis of gaussian-shaped profiles.

This result confirms the validity of the corrections for interference in substances similar to those we ex-

(17) H. P. Klug, L. E. Alexander, *X-ray diffraction procedures*, Wiley, New York, 1959, p. 512.
(18) H. D. Megaw and A. R Stokes, *J. Inst. Metals*, *71*, 6 (1945).
(19) W. H. Hall, *Proc. Phys. Soc. (London)*, *A 62*, 741 (1949).
(20) B. E. Warren, *Progress in Metal Physics*, *8*, 147 (1959).
(21) E. R. Boyko, J. D. Eichenberg, R. B. Roof, and E. K. Haltemann, *USAEC Rpt. WAPD-BT*, 128 (1959).
(22) A. R. Stokes, *Proc. Phys. Soc. (London)*, *A 61*, 382 (1948).
(23) C. N. J. Wagner and E. N. Aqua, *Advances in X-Ray Analysis*, *7*, 46 (1963).

amined, for which neither the retransformation in sol nor the dispersion in ultrafine form into a proper diluent is possible.

In general the values found at small angles are slightly lower than the wide-angle measurements, but they follow the same pattern. Among the possible sources of error, we have here to remember the approximation of employed mathematical formulas, the unavoidable imperfections in camera alignment, which of course have some influence at very small angles, and in particular the difficulty of carrying out accurate density measurements on highly lyophilic gels.

Analysis of radial distribution function. The aim of this section of the research was to confirm the existence of eventual intermediate forms between hydroxides and oxides, starting from the hypothesis that these may not be obtained in the crystalline state, that is long-range ordered.

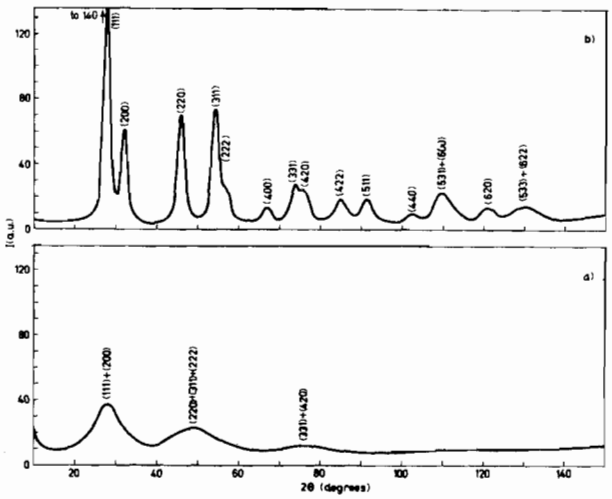

Figure 1. X-ray diffraction spectra (CuKα radiation) for the samples: a) LC; b) HC/400°.

In Figure 1 the indicative diffraction spectra are reported of widely differing samples of the significant series we have examined by this technique, that is LC and HC/400°. The intermediate samples show of course diffractograms with features gradually variable between these two extremes. Since the « infinite » thickness conditions are fulfilled because of the high absorption coefficient of the samples, we have applied only corrections for instrumental background and polarization; the conversion to an absolute scale of intensities I_{eu} (s) (where $s = 4\pi \sin\theta/\lambda$) was performed taking into account the fact that coherent intensity, at large enough *s* values (between 7 and 8), practically coincides with total independent scattering from various atoms.

In the present case of polyatomic substances, we use the approximated formula for the atomic scattering factor of an atom type m:

$$f_m = K_m f_e \qquad (9)$$

where f_e is an average unit electronic scattering factor for the repeat group of atoms considered, K_m is a constant which is characteristic of every atomic species and is equal to the atomic number Z_m for unionized atoms; if the atom is ionized, K_m is then the actual number of electrons present in the atom.

For f_e we can write:

$$f_e = \frac{\sum_m f_m}{\sum_m Z_m}$$

If we indicate the electronic density distribution function by g(r), the expression of average diffracted intensity becomes in this case:

$$\bar{I}(s) = N\left\{\sum_m f_m^2 - 4\pi f_e^2 \int_0^\infty \sum_m K_m [g_o - g_m(r)] r^2 \frac{\sin sr}{sr} dr\right\} \qquad (10)$$

where N is the number of repeat groups (or molecules) which contribute to the diffraction phenomenon, $g_m(r)$ is the electronic density function to be determined and g_o is the average value of this density, that is the average number of electrons per unit volume.

Applying the Fourier transformation to (10), we obtain the basic relation:

$$4\pi r^2 \sum_m K_m g_m(r) = 4\pi r^2 g_o \sum_m K_m + \frac{2r}{\pi} \int_0^\infty s \; i(s) \sin rs \; ds \qquad (11)$$

where:

$$i(s) = \frac{\bar{I}(s)/N - \sum_m f_m^2}{f_e^2} = \sum_m K_m^2 \left(\frac{\bar{I}(s)}{N \sum_m f_m^2} - 1 \right) \qquad (12)$$

this i(s) takes the meaning of a true interference function, as it represents the oscillating part of the average diffracted intensity, superimposed on the monotonically decreasing one in function of *s*, due to independent scattering.

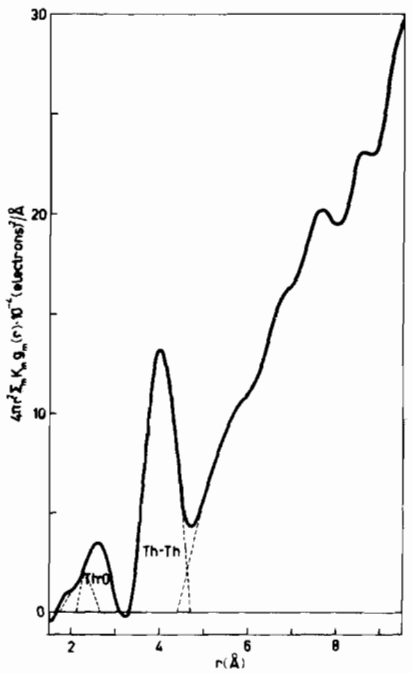

Figure 2. Experimental radial electronic distribution function for sample LC.

In order to limit the errors produced by truncation of the series, we have of course applied the usual correction factor to i(s), named « artificial temperature factor », in the form $\exp(-ps^2)$; the most satisfactory value for the damping constant p in order to obtain a good resolution of maxima has been evaluated from:

$$\exp(-ps^2_{max})=0.5$$

All the calculations have been carried out with the aid of a computer and the experimental radial distribution functions obtained in electronic units on the basis of a ThO_2 simplified unit of composition and accounting for ionization by employing Th^{4+}(86) and O^{2-} (10) scattering factors are represented in Figures 2-6.

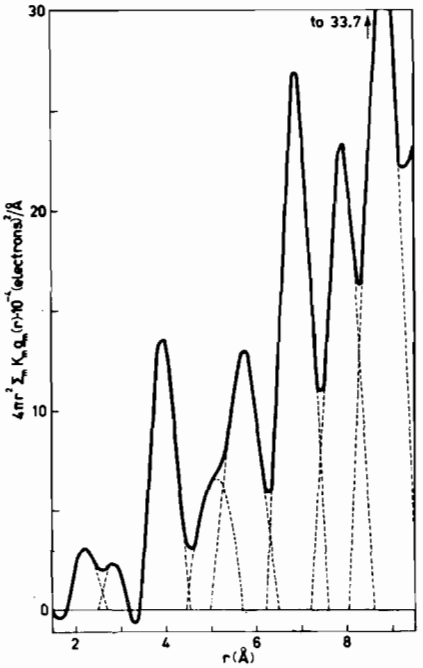

Figure 3. Experimental radial electronic distribution function for sample MC.

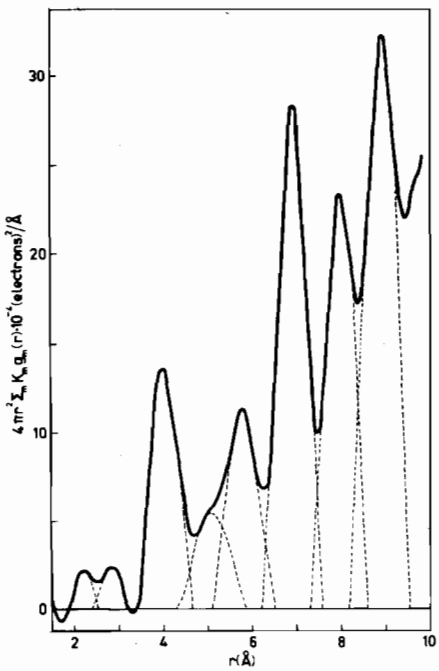

Figure 4. Experimental radial electronic distribution function for sample HC.

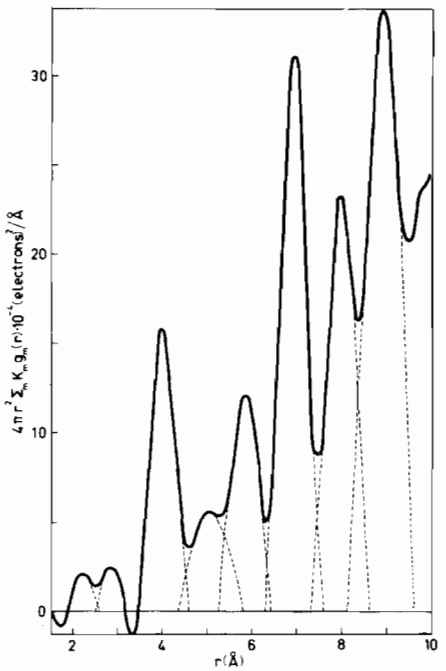

Figure 5. Experimental radial electronic distribution function for sample HC/120°.

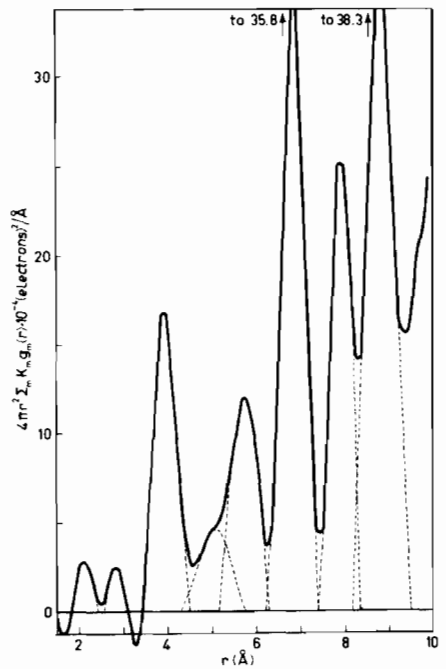

Figure 6. Experimental radial electronic distribution function for sample HC/400°.

The part of the curve below $r=1.5$ Å has been omitted because it is strongly affected by spurious effects and furthermore not significant for the purposes of this work.

Table V. Results of the analysis of radial distribution curves for Thoria gels and comparison with crystalline ThO_2 structural model

crystalline ThO_2				LC		MC		HC		HC/120°		HC/400°	
r_{calc}(Å)	interatomic distances	number of coordinated atoms	$(el)^2_{calc} \cdot 10^{-3}$	r_{obs}(Å)	$(el)^2_{obs} \cdot 10^{-3}$	r_{obs}(Å)	$(el)^2_{obs} \cdot 10^{-3}$	r_{obs}(Å)	$(el)^2_{obs} \cdot 10^{-3}$	r_{obs}(Å)	$(el)^2_{obs} \cdot 10^{-3}$	r_{obs}(Å)	$(el)^2_{obs} \cdot 10^{-3}$
2.42	Th-O	8	13.76	2.23 (1.75-2.66)	9.7	2.22 (1.77-2.70)	17	2.21 (1.86-2.55)	10	2.20 (1.85-2.56)	10	2.13 (1.81-2.44)	11
2.80	O-O	6	1.2	2.60 (2.13-3.10)	20.7	2.84 (2.50-3.17)	10	2.86 (2.43-3.23)	12	2.86 (2.50-3.15)	10	2.86 (2.58-3.09)	8
2.80(*)	Th-O(*)	6(*)	10.3(*)										
3.96	Th-Th	12	88.75	4.01 (3.30-4.68)	101	3.96 (3.40-4.55)	88	4.00 (3.37-4.64)	95	3.98 (3.44-4.57)	102	3.94 (3.43-4.51)	106
3.96	O-O	12	2.4										
4.64	Th-O	24	41.28										
4.85	O-O	8	1.6	not resolved	—	5.12 (4.48-5.73)	56.4	5.07 (4.26-5.87)	52	5.07 (4.34-5.80)	51	5.10 (4.36-5.75)	39
4.85(*)	Th-O(*)	8(*)	13.76(*)										
5.60	Th-Th	6	44.38			5.80 (5.02-6.50)	112.5	5.80 (5.13-6.47)	95	5.83 (5.26-6.40)	82	5.76 (5.20-6.35)	83
5.60	O-O	6	1.2	5.85	not det.								
6.10	Th-O	24	41.28										
6.25	O-O	24	4.8	not resolved	—	—	—	—	—	—	—	—	—
6.25(*)	Th-O(*)	24(*)	41.28(*)										
6.86	Th-Th	24	177.6	6.90	not. det.	6.93 (6.26-7.60)	203.5	6.91 (6.24-7.56)	208	6.92 (6.28-7.55)	210	6.88 (6.28-7.41)	217
6.86	O-O	24	4.8										
7.27	Th-O	32	55			7.93 (7.26-8.60)	179	7.96 (7.32-8.61)	177	7.94 (7.32-8.54)	167	7.93 (7.41-8.40)	143
7.92	Th-Th	12	88.75	7.66	not. det.								
7.92	O-O	12	2.4										
8.30	Th-O	48	82.56	not resolved	—	—	—	—	—	—	—	—	—
8.40	O-O	24	4.8										
8.40(*)	Th-O(*)	24(*)	41.28(*)			8.86 (8.10-9.70)	300	8.90 (8.23-9.56)	264	8.88 (8.13-9.60)	283	8.83 (8.18-9.50)	285
8.85	Th-Th	24	177.6	8.63	not det.								
8.85	O-O	24	4.8										
9.10	Th-O	24	41.28										

Notes: values marked by (*) represent Th—O distances not present in ThO_2 fluorite type structure. Intervals of r in brackets, under the value corresponding to the maximum, indicate lateral extent of the peak, schematized as a gaussian curve, and allow to value the overlappings of unresolved maxima.

In Table V are reported the interatomic distances derived from these diagrams, the maximum areas expressed in (electrons)^2 and the comparison with the theoretical model calculated from the crystalline ThO_2 structure, on the basis of number of atoms coordinated at various distances.[24]

Results and Discussion

The structures of different thoria sols obtained from $Th(NO_3)_4$ by a hydrolysis process which leads from 0 to 3 OH^- anions per thorium atom, have been studied by Johansson[25] through radial distribution analysis. In the group of diagrams regarding these sols, the peaks at 4 Å have been assigned by the author to Th—Th distances, with maximum coordination number of about 3, while peaks at about 2.5, 4.5, and 6.5 Å are associated to Th—O distances.

The proposed model for molecular species present in the solution, is a tetrahedral compound formed by combination of two dinuclear complexes[26] in which each thorium atom is surrounded by two oxygen atoms at about 2.6Å and by another thorium atom at 4 Å, to which it is bound by a double oxygen bridge.

The most hydrolyzed solutions show a hint of peak at 7.6 Å which cannot be explained by this model, but only with the coexistence of more condensed complexes, so that the maximum at 6.5 Å would be partially associated with Th—Th distances. A similar tetrahedral model has been also proposed by Bacon and Brown[27] for aqueous solutions of thorium perchlorate. However, in the gels we have studied, peaks at about 4.0, 6.9, and 7.9 Å may be assigned to Th—Th distances and are very close to positions and areas of Th—Th peaks of crystalline ThO_2, if we take account of partial overlappings of several maxima, some of which are not resolved.

Even in the gels of lowest crystallinity, maxima due to further Th—Th distances at about 5.8 and 8.8 Å are clearly detectable, that fit in the crystalline thorium oxide model. We emphasize that the *r* value corresponding to the first maximum due to Th—O distances in experimental curves is lower than the calculated value because of series truncation error which is not completely removed. We have chosen a lower damping constant *p* to avoid an excessive worsing in the peak resolution at larger *r* values.

In all diagrams a clean and well resolved peak at 2.60-2.86 Å is present, whose area does not agree with the fluorite type structure of ThO_2, since the interstitial sites in (0,0,½) positions, that is at 2.8 Å from thorium atoms, are not in those sterical conditions to be able to lodge hydroxyl groups or water molecules in such quantities, even admitting an association in zones of interstitial oxygen atoms and anionic vacancies, like that found by Willis[28] in some hyperstoichiometric uranium oxides.

Studies of thoria gel by means of infrared spectroscopy[29] have shown the presence of various forms of surface water physically adsorbed and other forms chemically bound, like hydroxyl groups, on the (100), (110), and (111) crystallographic planes. Examinations by electron diffraction show that the latter seem to be prevalent.

According to such a model, one could find some isolated surface hydroxyl groups, coordinated to underlying thorium cations and to oxygen anions situated in a still lower level. The distance between surface Th^{4+} and OH^- has a value equal to half the unit cell parameter.

The presence of these surface hydroxyl groups, together with O—O distances in gel and in water,[30] can

(24) R. Zannetti and G. Celotti, *Elementi di Strutturistica Chimica Diffrattometrica*, Piccin, Padova, 1969, p. 312.
(25) G. Johansson, *Acta Chem. Scand.*, *22*, 399 (1968).
(26) G. Johansson, *ibidem*, *22*, 389 (1968).
(27) W. E. Bacon and G. H. Brown, *J. Phys. Chem.*, *73*, 4163 (1969).
(28) B. M. T. Willis, *IAEA Tech. Rpt.*, *39*, 7 (1965).
(29) C. S. Olsen, M. E Wadsworth, and F. H. Olson, *UCNC Tech. Rpt.* TID 23957, XXX (1967).
(30) J. Morgan and B. E. Warren, *J. Chem. Phys.*, *6*, 666 (1938).

explain the peak we found at 2.8 Å and its relatively high area, and further it justifies the displacement of the second Th–O peak from the 4.64 Å value of ThO_2 to 5.1 Å ($\cong\sqrt{3}/2\ a$); it explains also the noticeable decrease in area of both as a function of annealing temperature.

The surface hydroxyl groups justify also the increase of unit cell parameter a through a surface tension phenomenon,[31,32] which could also be possible through the effect of lattice disorder.[33] This parameter increases up to 5.63 Å for LC sample, compared with $a=$ 5.595 Å given by literature for crystalline ThO_2.[34] Other more crystalline samples show a values gradually decreasing towards this second one.

It is scarcely probable that residual surface nitrates can contribute to the peak at 2.8 Å, either because the peak still remains after 400°C thermal treatment, or because in this case the distance would be of about 3.1Å.[26] It is likely that one can exclude the presence of carbonates coming from atmospheric CO_2.

The maxima in the diagrams referring to HC/120° and HC/400° samples can be explained either through the presence of surface hydroxyl groups bound up to such temperatures or through that of quickly adsorbed water before X-ray diffraction measurements. To decide in this regard we deem to be necessary a diffractometric examination by a high-temperature camera. In the five samples examined, the peak at 2.8 Å decreases with increasing crystallinity and annealing temperature; this fact may be associated with the consequences of decreasing number of present OH^-, produced by the lowering of surface/volume ratio in gel with increasing temperature. One has to note that for the sample annealed at 400°C, the areas of peaks at 2.8 and 5.1 Å undergo a more marked decrease; the partial disappearing of adsorbed water contributes to this phenomenon, already ascertained,[29] by annealing beyond 200°C, and the rising of oxygen bridges between hydroxyl groups located on opposite interfaces of adjacent particles.

In conclusion, we have evaluated the average particle dimensions by a very valid method, although we were dealing with very densely packed materials, since we have applied the interference term correction. Particle sizes coincide very nearly with crystallite ones. It is also found from elongation measurements,[11,15] that particles tend towards a spherical shape and, in unannealed or gels annealed at low temperature, the dimensions show slight deviations from the average values (see Tables II, III, and IV). The particles are essentially oxide, even if lattice order is not high.

We have not found the presence of intermediate forms between oxides and hydroxides, of different structures. On the surface of the particles, adsorbed water and hydroxyl groups are present; the location of the last, that was not unequivocal from the interpretation of infrared peaks, results determined in the (0,0,½) interstitial positions; therefore each surface thorium atom on (100) faces coordinates 4 hydroxyl groups, 4 on (110) faces and 3 on (111) faces, as is shown in Figures 7-9; to these they have to be added the molecules of adsorbed water located at about the same distance, *i.e.* at nearly 2.8 Å, on a more external layer and which contribute also to the formation of bonds between different particles. The faces belonging to the three types (100), (110), and (111) are all present exactly because of the almost spherical shape of particles (see Figure 10): the total coordination

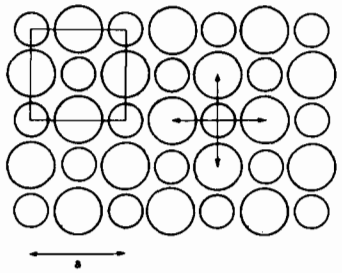

Figure 7. Schematical drawing of the (100) surface of the particle: small circles represent torium iohns, large circles hydroxyl groups on the considered surface. Hydroxyl groups marked with arrows are at a distance of 2.8 Å from thorium ion included between them.

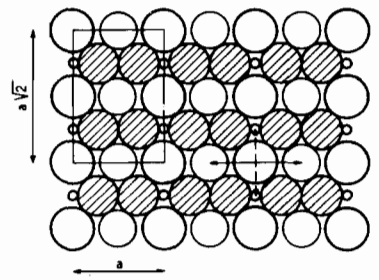

Figure 8. Schematical drawing of the (110) surface of the particle: blank large circles represent thorium ions, shaded circles oxygen ions on the surface, blank medium circles hydroxyl groups on the surface and blank small circles hydroxyl groups on a plane external to the surface, lying at a distance of $\frac{\sqrt{2}}{4}a$ from (110) plane. Hydroxyl groups marked with arrows are at a distance of 2.8 Å from thorium ion included between them.

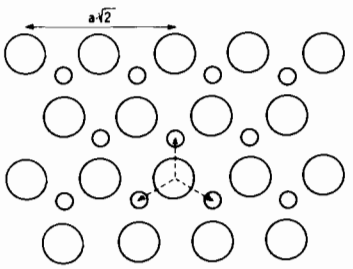

Figure 9. Schematical drawing of the (111) surface of the particle: large circles represent thorium ions, small circles hydroxyl groups on a plane external to the surface, lying at a distance of $\frac{\sqrt{3}}{4}a$ from (111) plane. Hydroxyl groups marked with arrows are at a distance of 2.8 Å from thorium ion included between them.

(31) D. T. Livey, B. M. Wanklin, M. Hewitt, and P. Murray, *Trans. Brit. Ceram. Soc.*, 56, 217 (1957).
(32) T. B. Rymer, *Nuovo Cimento*, 6, (Suppl 10), 294 (1957).
(33) A. Cimino, P. Porta, and M. Valigi, *J. Am. Ceram. Soc.*, 49, 152 (1966).
(34) B. J. Skinner, *Am. Mineral.*, 42, 39 (1957).

number for each surface thorium atom is about 5 in respect to oxygen. In the radial distribution curves the peak at 2.8 Å is large owing also to the great value of the ratio between the numbers of surface OH^- and oxygen ions of oxide, due to the high specific surface.

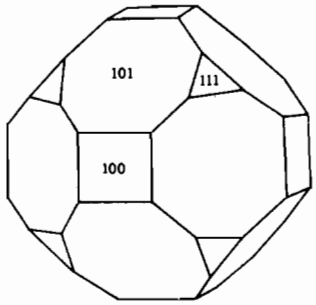

Figure 10. Model for one of the possible shapes of particles.

Acknowledgements. The authors thank Prof. G. Semerano, Director of the « G. Ciamician » Chemical Institute of University of Bologna, for his promoving and encouraging collaboration between various departments, so making possible the execution of this work, and for the critical discussion of the same, the researchers and technicians of the Laboratory of Industrial Chemistry of C.N.E.N. - Casaccia and in particular Dr. A. Bazzan, for preparation, treatments and some analyses of samples and for discussion of the results.